due to acute pump failure or lethal arrhythmias. After MI was produced, rats were randomly selected for death at various time points.

Determination of infarct size. The rats were anesthetized with pentobarbital, and their hearts were arrested with potassium chloride and rapidly excised. After body weight and heart weight were measured, three thin transverse slices were cut from the apex to base, and these were embedded with an OCT compound (Miles, Elkhart, IN) and were frozen in liquid nitrogen. The infarct size was determined using the triphenyltetrazolium chloride (TTC) staining method as described previously (1, 26). Rats with infarcts occupying <35% of the left ventricle were excluded from the analysis because less significant cardiac remodeling was expected in rats with small-sized MI. Roughly 10% of animals were excluded based on this criteria.

Echocardiographic studies. To evaluate the left ventricular dimensions and function, transthoracic echocardiography (Hewlett-Packard, Palo Alto, CA) was performed at each time point with a 7.5-MHz sector scan probe. M-mode echocardiograms at the papillary muscle level were recorded using two-dimensional long-axis images as a guide under mild anesthesia with pentobarbital (15 mg/kg im). The left ventricular end-diastolic and end-systolic dimension was measured from the M-mode tracing. The left ventricular fractional shortening was calculated as described previously (1, 26). The systolic blood pressure of each animal was measured before echocardiographic studies by the tail-cuff method.

Western blot analysis. For all Western blot analyses, noninfarct myocardial tissue samples were obtained. Lysates (60 μg) from heart tissues, or the immunoprecipitates, were separated by a 10% SDS-polyacrylamide gel electrophoresis, and the separated proteins were transferred to a polyvinylidene difluoride membrane (Millipore, Billerica, MA). The membranes were immunoblotted with anti-TGF-β1, -TβRI, -TβRII, -TAK1, -MKK3/6, -phosphorylated MKK3/6 (P-MKK3/6), -p38 MAPK, or -phosphorylated p38 MAPK (P-p38) antibodies (Santa Cruz Biotechnology, Santa Cruz, CA) using an enhanced chemiluminescence detection system (Amersham, Piscataway, NJ).

In vitro kinase assay. The amount of activated form of TAK1 was measured by in vitro kinase assay (11); lysates from noninfarct myocardium were immunoprecipitated by anti-TAK1 antibody, and the immunoprecipitates were then incubated with recombinant MKK3/6 (Upstate Biotechnology, Lake Placid, NY) (20 μg/ml) and 100 μM [γ-^{32}P]ATP (1 μC) in a solution containing 20 mM Tris-Cl, pH 7.5, 2 mM EGTA, and 10 mM $MgCl_2$ for 20 min at 30°C. The reaction was stopped by boiling the samples. After SDS-polyacrylamide gel electrophoresis, phosphorylation of MKK3/6 was detected by autoradiography.

Immunoprecipitation was carried out as follows: noninfarct myocardial tissue samples were homogenized with a tissue homogenizer in a lysis buffer (50 mM Tris-Cl, pH 7.4; 150 mM NaCl; 1% NP-40; 0.25% sodium deoxycholate; 1 mM EDTA; 2 μM leupeptin; 1 μM PMSF). The debris was removed by centrifugation at 1,000 *g* for 15 min. The protein concentration of the lysates was determined with the Bradford protein assay (Bio-Rad, Hercules, CA). Lysates were incubated with an anti-TAK1 antibody (Santa Cruz Biotechnology) and protein A-sepharose (Amersham) for 3 h at 24 C. The immunoprecipitates were washed three times and eluted with 20 μl of sample buffer (62.5 mM Tris, pH 6.8; 2% SDS; 20 mM DTT; and 1% glycerol).

Real-time RT-PCR. For analysis of mRNA levels for TAK1, TβRI, TβRII, ANP, and β-MHC, total RNA was isolated from myocardial tissue samples by use of the RNeasy Mini Kit (Qiagen, Valencia, CA). Subsequently, DNase-treated total RNA was reverse-transcribed by use of SuperScriptIII FirstStrand Synthesis System (Invitrogen, Carlsbad, CA). Measurements of mRNA levels were performed by real-time reverse transcription-polymerase chain reaction (RT-PCR) by use of an ABI PRISM 7900HT Sequence Detection System (Applied Biosystems, Foster City, CA). A 25-μl reaction mixture was used that contained 12.5 μl SYBR Green PCR Master Mix (Applied Biosystems), 10 ng of cDNA template, and the following primers: 5′-CGCCATCGCAGGTCCTTAAC-3′ (sense), 5′-GGCTGCATGCTGTGCAGGTA-3′ (antisense) for TAK1; 5′-GGACTTGCTGTGAGACATGA-3′ (sense), 5′-CATGCTGCTCCATTGGCATA-3′ (antisense) for TβRI; 5′-TTCACCTACCACGGCTTCAC-3′ (sense), 5′-CAGGATGATGGCGCAGTTGT-3′ (antisense) for TβRII; 5′-TATACAGTGCGGTGTCCAAC-3′ (sense), 5′-GCTCCAATCCTGTCAATCCT-3′ (antisense) for ANP; 5′-GAAGGAGATGGCCAACATGA-3′ (sense), 5′-AGCTCTGAGCACTCGTCTTC-3′ (antisense) for β-MHC; and 5′-ACCACAGTCCATGCCATCAC-3′ (sense), 5′-TCCACCACCCTGTTGCTGTA-3′ (antisense) for glyceraldehyde-3-phosphate dehydrogenase (GAPDH). In each experiment, a standard curve for each primer pair was obtained using a serial dilution of a recombinant plasmid containing cDNA. The threshold cycle (Ct) was subsequently determined. Relative mRNA levels were calculated based on the Ct values and normalized by the GAPDH level of each sample. To avoid the possibility of amplifying contaminating DNA, all the primers for real-time RT-PCR were designed with an intron sequence inside the cDNA to be amplified, and reactions were performed with appropriate negative control samples (template-free control samples).

Immunohistochemistry. The avidin-biotin peroxide complex technique was used. Five-micrometer-thick sections were cut from heart tissues surrounded with the OCT compound and fixed with 2% paraformaldehyde. Intrinsic peroxidase activity was blocked with 0.25% H_2O_2. The sections were blocked with 5% bovine serum albumin and then incubated at 4°C with the anti-TβRI, -TβRII, or -TAK1 antibody overnight. After a wash with TTBS (0.1% Tween 20, 0.9% NaCl in 0.1 M Tris-Cl, pH 7.4), a biotinylated anti-rabbit or -mouse IgG antibody was added, and incubation was carried out with a streptavidin-peroxidase complex (Vector Laboratories, Burlingame, CA). Peroxidase activity was detected by using 3,3′-diaminobenzidene, and slides were then counterstained with hematoxylin.

Statistics. Values are presented as means ± SE. The measurements from rats with MI were compared with those of sham-operated rats by using Student's unpaired *t*-test. The significance of difference among the means of various groups was analyzed by one-way ANOVA with post hoc comparisons by using the Tukey-Kramer test. Significance was taken as $P < 0.05$.

RESULTS

Body and heart weights and infarct size. Table 1 shows body and heart weight and infarct size of animals after the sham operation and after 1, 3, 7, and 14 days of MI. The heart weight and the heart-to-body weight ratio of the MI group 3 days postinfarct, by which time inflammation and edema had developed within the infarct, significantly increased ($P < 0.05$) compared with those of the sham-operated control group and then returned to the control values 7 days postinfarct and thereafter. All animals developed large MIs, with infarct size (determined by TTC staining) ranging from 37.7% to 52.8% of the left ventricle, and these values did not change significantly over the experimental period (by 14 days postinfarct).

Hemodynamics and echocardiographic study. Rats with MI exhibited progressive left ventricular remodeling, both hemodynamically and geometrically. Table 2 represents the hemodynamic parameters and echocardiographic data in sham-operated rats and those after 1, 3, 7, and 14 days of MI. In all of the animals with MI compared with the sham-operated animals, blood pressure was significantly lower, and heart rate was significantly higher at all time points.

Left ventricular diastolic and systolic dimensions increased rapidly during the acute phase of MI, and progressive changes

Table 1. *Body weight, heart weight, and MI size of rats with MI and of sham-operated controls*

	Time Postinfarct, days				
	0	1	3	7	14
Body wt, g					
MI	322±2	283±1	281±2	293±2	330±2
Sham operated	321±4	285±2	292±4	299±2	325±3
Heart wt, mg					
MI		854±3	889±5†	862±7	965±7
Sham operated		857±6	860±10	870±5	972±7
Heart wt/body wt, mg/g					
MI		3.02±0.01	3.21±0.02*	2.94±0.01	2.93±0.01
Sham operated		3.03±0.01	2.95±0.02	2.92±0.01	2.99±0.03
MI size, %					
MI		47.9±2.0	48.6±1.2	50.9±1.0	47.1±2.4
No. of rats					
MI	25	25	17	16	13
Sham operated	14	14	12	9	8

Values are means ± SE. MI, myocardial infarction. *$P < 0.01$, †$P < 0.05$, infarct group compared with respective noninfarcted control group at each time point.

were observed by 2 wk ($P < 0.01$ at each time point compared with sham-operated rats). In parallel, fractional shortening decreased rapidly during the acute phase due to akinesis of the anterior wall, and this systolic dysfunction persisted thereafter ($P < 0.01$ at each time point compared with sham-operated rats). Posterior wall thickness was significantly ($P < 0.01$) increased in rats with MI compared with sham-operated rats on *day 3* and thereafter, which is a manifestation of compensated hypertrophy of noninfarct myocardium.

Western blotting of TGF-β1, TβRI, TβRII, TAK1, MKK3/6, P-MKK3/6, p38 MAPK, and P-p38 MAPK. Protein levels of components of the TGF-β1-TAK1-p38 MAPK pathway were determined by using Western blotting. TGF-β1 protein levels were increased compared with those in sham-operated rats by 1.30 ± 0.01-, 2.59 ± 0.10-, 2.34 ± 0.06-, and 1.57 ± 0.03-fold ($P < 0.01$) at 1, 3, 7, and 14 days after MI, respectively (Fig. 1, *A* and *B*). TβRI and TβRII expression showed modest but significant upregulation, peaking at 3 days after MI (Fig. 1, *A*, *C*, and *D*).

In parallel with the upregulation of TGF-β1, the protein levels of TAK1 were significantly increased 1.66 ± 0.14-, 1.97 ± 0.16-, and 1.57 ± 0.07-fold ($P < 0.01$) at 1, 3, and 7 days post-MI compared with sham-operated rats (Fig. 2, *A* and *B*). Although there was no change in the protein levels of MKK3/6 and p38 MAPK levels throughout the time course, P-MKK3/6 and P-p38 MAPK were increased significantly (P-MKK3/6: 2.20 ± 0.19-, 2.55 ± 0.47-, and 3.29 ± 0.32-fold; P-p38 MAPK: 1.90 ± 0.03-, 2.03 ± 0.06-, and 2.35 ± 0.06-fold at 1, 3, and 7 days after MI), indicating the activation of the TGF-β1-TAK1-MKK3/6-p38 MAPK pathway (Fig. 2,

Table 2. *Systolic BP, HR, left ventricular dimension, and fractional shortening of rats with MI and of sham-operated controls*

	Time Postinfarct, days				
	0	1	3	7	14
Systolic BP, mmHg					
MI	128±1	106±1*	109±1*	115±1*	126±1*
Sham operated	127±1	125±2	117±2	131±1	134±1
HR, beats/min					
MI	372±2	473±3*	396±4*	389±4*	380±4
Sham operated	366±3	398±7	368±3	372±3	376±4
LVDd, mm					
MI	5.9±0.1	6.9±0.1*	7.1±0.1*	7.3±0.1*	7.8±0.1*
Sham operated	6.0±0.1	6.0±0.1	6.0±0.1	6.2±0.1	6.4±0.1
LVDs, mm					
MI	3.4±0.1	5.2±0.1*	5.5±0.1*	5.6±0.1*	5.9±0.1*
Sham operated	3.4±0.1	3.5±0.1	3.7±0.1	3.8±0.1	3.9±0.1
PWT, mm					
MI	1.3±0.1	1.3±0.1	1.4±0.1*	1.4±0.1*	1.5±0.1*
Sham operated	1.3±0.1	1.3±0.1	1.3±0.1	1.3±0.1	1.4±0.1
FS, %					
MI	42.9±0.3	24.4±0.7*	22.6±0.5*	23.2±0.3*	24.6±0.5*
Sham operated	43.2±0.4	40.6±0.6	38.4±0.6	39.0±0.4	39.6±0.5
No. of rats					
MI	25	25	17	16	13
Sham operated	14	14	12	9	8

Values are means ± SE. BP, blood pressure; HR, heart rate; LVDd, left ventricular diastolic dimension; LVDs, left ventricular systolic dimension; PWT, posterior wall thickness; FS, fractional shortening. *$P < 0.01$, infarct group compared with respective noninfarcted control group at each time point.

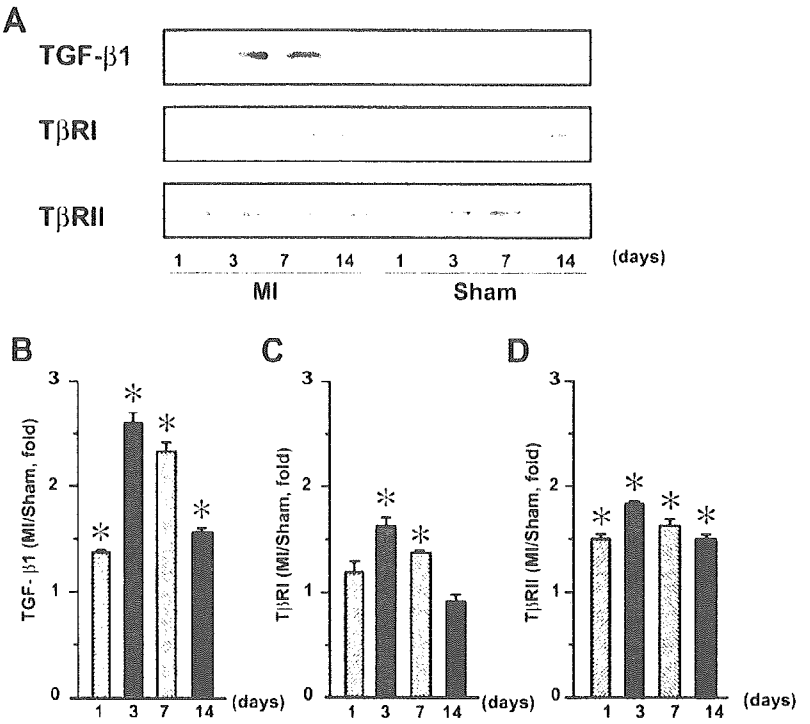

Fig. 1. Representative Western blotting of transforming growth factor-β1 (TGF-β1) and TGF-β receptor types I and II (TβRI and TβRII) in the noninfarcted myocardium (*A*). Densitometric analyses of the blot show that TGF-β1 and TβRII expression was increased compared with sham-operated rats 1, 3, 7 and 14 days after myocardial infarction (MI) (*B* and *D*). The expression level of TβRI was also increased 3 and 7 days postinfarct (*C*). Number of samples for each group is 6. $^*P < 0.01$.

A, *C*, and *D*). At 14 days postinfarct, all of these returned to the control level (Fig. 2, *A–D*).

In vitro kinase assay. To directly demonstrate that TAK1 is activated in post-MI remodeling and is capable of activating the downstream substrates MKK3/6-p38 MAPK, we performed an in vitro kinase assay. Recombinant MKK3/6 was coincubated with heart protein samples immunoprecipitated by TAK1 antibody. As shown in Fig. 2*E*, phosphorylation of MKK3/6 was increased in animals with MI at 3 days postinfarct, a time when the TAK1 protein level reached a maximum.

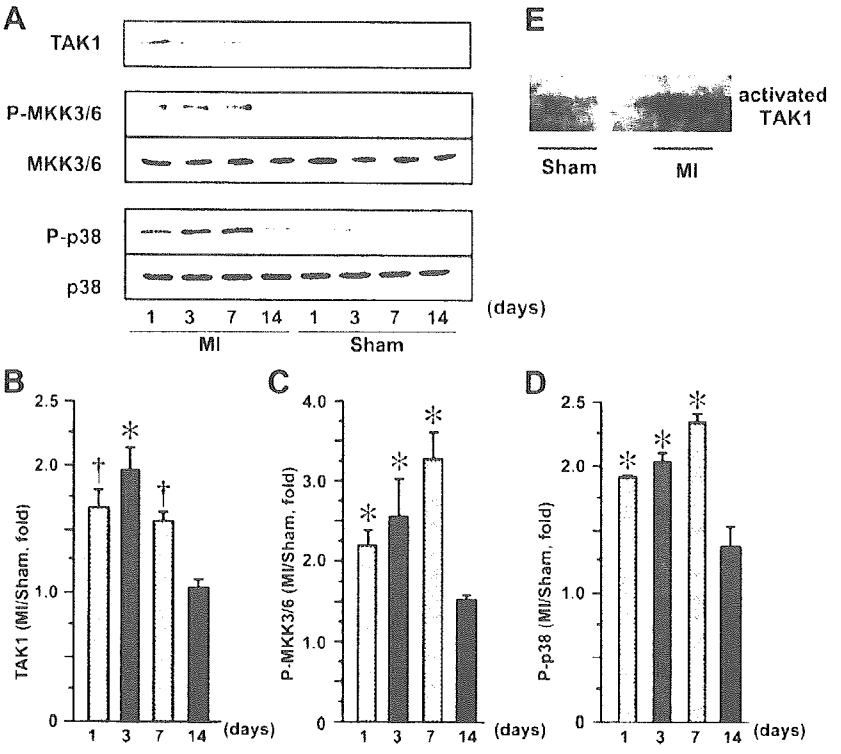

Fig. 2. Representative Western blotting of TGF-β-activated kinase (TAK1), MKK3/6, and p38 MAPK in the noninfarcted myocardium (*A*). Densitometric analyses of the blot show that expression of TAK1 was increased at 1, 3 and 7 days postinfarct (*B*). Although the expression levels of MAPKK 3/6 (MKK3/6) and p38 MAPK did not change after infarction, phosphorylated (P-) MKK3/6 and p38 MAPK levels were increased compared with sham-operated rats 1, 3, and 7 days after MI (*C* and *D*). Number of samples for each group is 6. $^*P < 0.01$, $^\dagger P < 0.05$. In vitro kinase assay demonstrates that TAK1 is activated in the post-MI remodeling heart, as shown by the augmented phosphorylation of recombinant MKK3/6, compared with that in control rats (*E*).

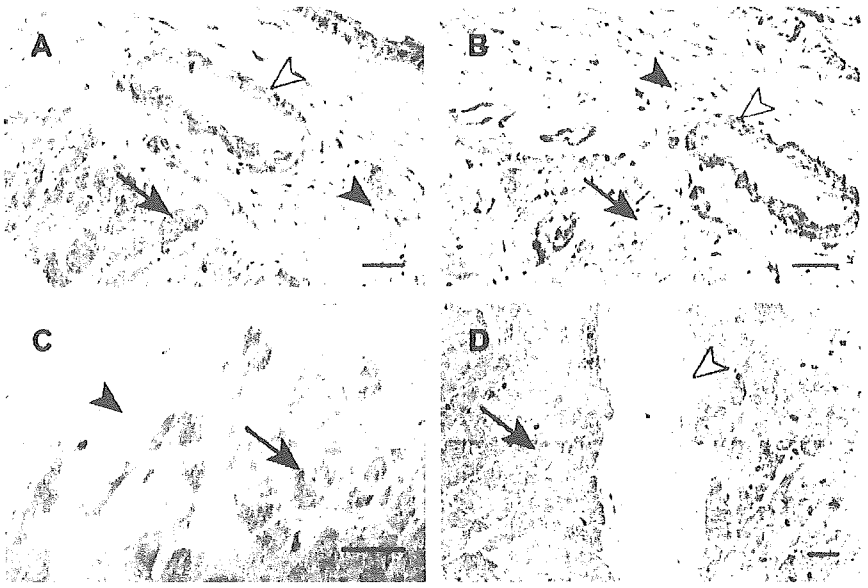

Fig. 3. Immunohistochemistry for TβRI, TβRII, and TAK1. Immunoreactivity for TβRI (*A*) and TβRII (*B*) was observed in fibroblasts (black arrowhead), vascular smooth muscle cells (white arrowhead), and cardiac myocytes (black arrow) of the border zone. In contrast, only cardiac myocytes were stained with anti-TAK1 antibody in the border zone (*C*) and in the noninfarcted region (*D*). All images were taken from tissue samples 3 days after MI. Bars, 20 μm.

Immunohistochemistry. We examined the localization of TβRI, TβRII, and TAK1 using immunohistochemical staining. Immunoreactive staining of TβRI (Fig. 3*A*) and TβRII (Fig. 3*B*) was observed in cardiomyocytes (black arrow), vascular smooth muscle cells (white arrowhead), and fibroblasts (black arrowhead) in the border zone of MI. In contrast, immunoreactivity for TAK1 was mainly localized to spared cardiomyocytes in the border zone of MI (Fig. 3*C*) and in the noninfarcted region (Fig. 3*D*), suggesting that the TGF-β1-TAK1 pathway was activated in cardiomyocytes but not in vascular smooth muscle cells or interstitial cells. In addition, TAK1 protein was not detected by Western blotting in the center of the infarcted region where there were no cardiomyocytes (data not shown).

mRNA levels of TAK1, TβRI, TβRII, ANP, and β-MHC. To determine whether the increases in TAK1 signaling occur at transcriptional level, we measured mRNA levels of TAK1,

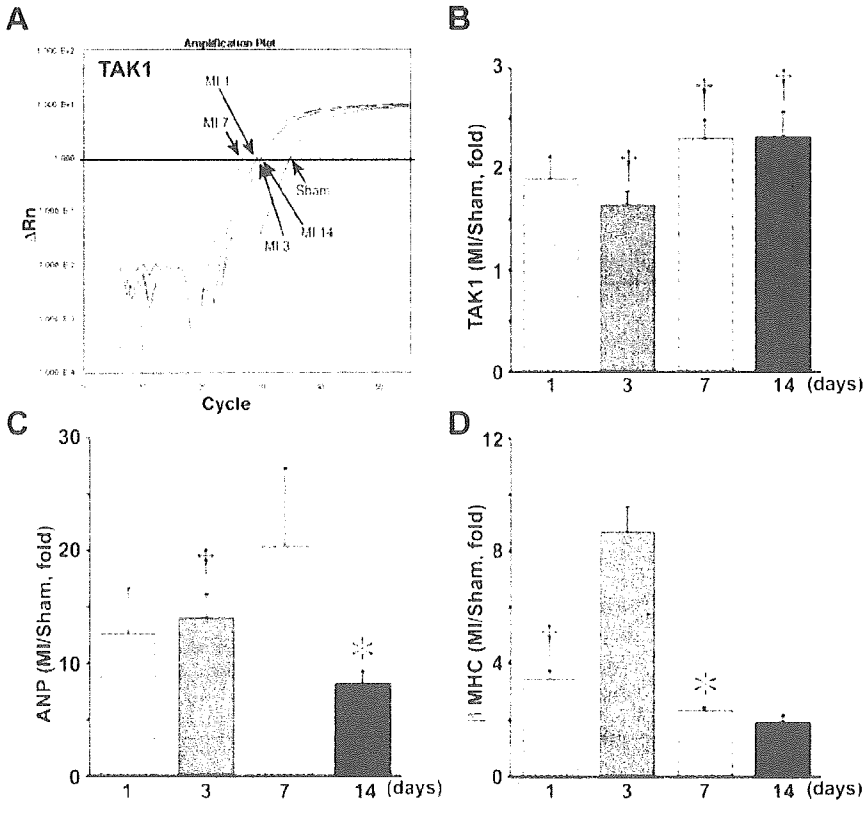

Fig. 4. Real-time RT-PCR for measurement of mRNA levels of TAK1 (*A* and *B*), atrial natriuretic peptide (ANP) (*C*), and β-myosin heavy chain (β-MHC) (*D*) in the noninfarcted myocardium. *A*: representative amplification curve of TAK1 from sham-operated rats and those with MI at various time points. *B*–*D*: summarized data at various time points. The data of each mRNA were normalized by their GAPDH mRNA and expressed as a fold increase compared with sham-operated rats. 1, 3, 7, and 14 days after MI. $^{*}P < 0.01$, $^{\dagger}P < 0.05$.

TβRI, and TβRII, using real-time RT-PCR (Fig. 4, *A* and *B*). It was previously reported that TGF-β1 mRNA is upregulated after MI (27, 29). TAK1 mRNA levels were increased by 1.91 ± 0.22-, 1.65 ± 0.12-, 2.30 ± 0.19-, and 2.33 ± 0.24-fold at 1, 3, 7, and 14 days after MI, respectively (Fig. 4*B*), compared with those in sham-operated rats. mRNA levels of TβRI and TβRII at 3 days after MI were 5.50- and 2.37-fold, respectively. Taken together, the increases in the signaling pathway were due to transcriptional upregulation.

To determine whether the expression of fetal cardiac genes was increased in the ventricles of rats after MI, we measured mRNA levels of ANP (Fig. 4*C*) and β-MHC (Fig. 4*D*) by real-time RT-PCR. Both ANP and β-MHC mRNA levels were increased compared with sham-operated rats at all time points (Fig. 4, *C* and *D*): 12.6 ± 3.9-, 14.0 ± 2.1-, 20.5 ± 6.9-, and 8.3 ± 1.0-fold for ANP, and 3.4 ± 0.3-, 8.7 ± 0.9-, 2.4 ± 0.1-, and 1.9 ± 0.3-fold for β-MHC at 1, 3, 7, and 14 days after MI, respectively. Thus profound upregulation of ANP and β-MHC mRNA levels was observed in the spared myocardium, indicating the presence of hypertrophic remodeling process in our MI model.

DISCUSSION

Here we demonstrated that the protein levels of TGF-β1, TβRI, TβRII, and TAK1 were significantly increased in the noninfarcted myocardium in rats with MI compared with sham-operated animals. Phosphorylation of MKK3/6 and of p38 MAPK was also increased in the noninfarcted region. This signaling cascade appeared to reach a maximum at *days 3–7* postinfarct and return to the control level by *day 14*. Moreover, activated TAK1 in noninfarcted myocardium was capable of activating recombinant MKK3/6, suggesting a causative role for TAK1 in the remodeling process. The immunoreactivity for TAK1 was mainly localized to cardiomyocytes, whereas that for TβRI and TβRII was observed in vascular smooth muscle cells and fibroblasts as well as cardiomyocytes. These lines of evidence suggest that the TGF-β1-TAK1-p38 MAPK pathway in cardiomyocytes of the noninfarcted region is activated during acute MI. In accordance with the activation of this pathway, ANP and β-MHC expression was increased. Although many trophic factors induce the expression of these genes, we clarified that TGF-β1 is one of the stimulators of cardiomyocyte hypertrophy during ventricular remodeling after acute MI and that this signal is transmitted through the TAK1-MKK3/6-p38 MAPK pathway.

Role of TGF-β1 in left ventricular hypertrophy and post-MI remodeling. TGF-β1 is a locally generated cytokine that has been implicated as a major contributor to tissue fibrosis in various organ systems (2). Studies with experimental models of MI and with pressure overload have shown increased myocardial TGF-β1 expression, suggesting the involvement of TGF-β1 in cardiomyocyte hypertrophy as well as fibrosis (3, 9, 25, 27, 29). Overexpression of TGF-β1 in transgenic mice results in interstitial fibrosis and hypertrophic growth of cardiomyocytes (18). TGF-β1 provokes the genetic upregulation of fetal contractile proteins, such as β-MHC and α-skeletal actin in cultured neonatal cardiomyocytes (15). However, the intracellular signaling pathway of TGF-β1-induced cardiomyocyte hypertrophy after MI has remained unknown. It has been demonstrated that activated MKK3/6-p38 MAPK induces the expression of genes encoding sarcomeric proteins and elicits sarcomeric organization in cultured cardiomyocytes (28, 31). In this study, we demonstrated that expression of TAK1, the stimulator of MKK3/6 in the signal transduction of TGF-β1, increased and the protein was localized to cardiomyocytes during acute MI.

TGF-β1 induced myocyte hypertrophy and collagen deposition. TGF-β1 induces extracellular matrix production in fibroblasts and promotes fibrosis. Two major signaling pathways, Smad proteins and TAK1, have been identified in the signal transduction of TGF-β1 in other types of cells (5, 8, 30). Smad signaling is particularly involved in collagen deposition in the extracellular matrix (17, 21). Indeed, the Smad pathway was also reported to be upregulated after MI in rats (7). Smad proteins were located mainly in the perivascular space in the noninfarcted region and in nonmyocyte cells, probably myofibroblasts, in the infarct scar. Although the role of Smad was not examined in these studies, Smad signaling seemed to play a major role in the elevated production of the extracellular matrix proteins in fibroblasts after MI. Although TGF-β1 was activated in both cardiomyocytes and fibroblasts after MI, the intracellular signaling pathways in these two distinct types of cells were different from each other. TAK1-p38 MAPK is activated in cardiomyocytes to induce myocyte hypertrophy.

Role of TAK1 in post-MI remodeling. Zhang et al. (32) reported that TAK1 is activated in cardiomyocytes after pressure overload. In transgenic mice with activated TAK1, considerable ventricular hypertrophy developed and led to impaired systolic and diastolic function. In this model, β-MHC mRNA expression was increased 20-fold compared with control mice. Comparable levels of β-MHC mRNA upregulation were observed in our rat MI model. The endogenous TAK1 may help to regulate β-MHC expression to prevent increased wall stress after MI. Although TAK1 was originally isolated as a target of TGF-β1 (30), TNF-α or IL-1 recently was also shown to activate TAK1 (13, 20). Given that TNF-α and IL-1 expression in the left ventricle is increased after MI (14), TNF-α or IL-1 may stimulate TAK1 in the cardiomyocytes during acute MI, although we did not determine the expression levels of these cytokines.

Pathophysiological implications. In conclusion, activation of the TGF-β1-TAK1-p38 MAPK pathway is at least one of the important responses to cardiac remodeling that is involved in the progression of heart failure. These observations suggest that this signaling pathway could be a novel therapeutic target for the suppression of post-MI remodeling. However, further studies are required to see whether the blockade of the TAK1-signaling pathway would lead to the inhibition of post-MI remodeling and subsequent heart failure.

ACKNOWLEDGMENTS

Present address of T. Aoyama: Kansai Electric Power Hospital, 2-1-7 Fukushima, Fukushima-ku, Osaka 553-0003, Japan.

GRANTS

This study was supported by grants-in-aid for scientific research from the Ministry of Education, Science, Sports and Culture, Japan, and a grant from the Japan Cardiovascular Research Foundation.

REFERENCES

1. **Aoyama T, Takimoto Y, Pennica D, Inoue R, Shinoda E, Hattori R, Yui Y, and Sasayama S.** Augmented expression of cardiotrophin-1 and

its receptor component, gp130, in both left and right ventricles after myocardial infarction in the rat. *J Mol Cell Cardiol* 32: 1821–1830, 2000.
2. **Border WA and Noble NA.** Transforming growth factor β in tissue fibrosis. *N Engl J Med* 331: 1286–1292, 1994.
3. **Casscells W, Bazoberry F, Speir E, Thompson N, Flanders K, Kondaiah P, Ferrans VJ, Epstein SE, and Sporn M.** Transforming growth factor-β_1 in normal heart and in myocardial infarction. *Ann NY Acad Sci* 593: 148–160, 1990.
4. **Cohn JN, Ferrari R, and Sharpe N.** Cardiac remodeling—concepts and clinical implications: a consensus paper from an international forum on cardiac remodeling. Behalf of an International Forum on Cardiac Remodeling. *J Am Coll Cardiol* 35: 569–582, 2000.
5. **Derynck R and Zhang YE.** Smad-dependent and Smad-independent pathways in TGF-β family signalling. *Nature* 425: 577–584, 2003.
6. **Deten A, Holzl A, Leicht M, Barth W, and Zimmer HG.** Changes in extracellular matrix and in transforming growth factor-β isoforms after coronary artery ligation in rats. *J Mol Cell Cardiol* 33: 1191–1207, 2001.
7. **Hao J, Ju H, Zhao S, Junaid A, Scammell-La Fleur T, and Dixon IM.** Elevation of expression of Smads 2, 3, and 4, decorin and TGF-β in the chronic phase of myocardial infarct scar healing. *J Mol Cell Cardiol* 31: 667–678, 1999.
8. **Heldin CH, Miyazono K, and ten Dijke P.** TGF-β signalling from cell membrane to nucleus through SMAD proteins. *Nature* 390: 465–471, 1997.
9. **Kuwahara F, Kai H, Tokuda K, Kai M, Takeshita A, Egashira K, and Imaizumi T.** Transforming growth factor-β function blocking prevents myocardial fibrosis and diastolic dysfunction in pressure-overloaded rats. *Circulation* 106: 130–135, 2002.
10. **Massague J.** TGFβ signaling: receptors, transducers, and Mad proteins. *Cell* 85: 947–950, 1996.
11. **Moriguchi T, Kuroyanagi N, Yamaguchi K, Gotoh Y, Irie K, Kano T, Shirakabe K, Muro Y, Shibuya H, Matsumoto K, Nishida E, and Hagiwara M.** A novel kinase cascade mediated by mitogen-activated protein kinase kinase 6 and MKK3. *J Biol Chem* 271: 13675–13679, 1996.
12. **Nian M, Lee P, Khaper N, and Liu P.** Inflammatory cytokines and postmyocardial infarction remodeling. *Circ Res* 94: 1543–1553, 2004.
13. **Ninomiya-Tsuji J, Kishimoto K, Hiyama A, Inoue J, Cao Z, and Matsumoto K.** The kinase TAK1 can activate the NIK-I κB as well as the MAP kinase cascade in the IL-1 signalling pathway. *Nature* 398: 252–256, 1999.
14. **Ono K, Matsumori A, Shioi T, Furukawa Y, and Sasayama S.** Cytokine gene expression after myocardial infarction in rat hearts: possible implication in left ventricular remodeling. *Circulation* 98: 149–156, 1998.
15. **Parker TG, Packer SE, and Schneider MD.** Peptide growth factors can provoke "fetal" contractile protein gene expression in rat cardiac myocytes. *J Clin Invest* 85: 507–514, 1990.
16. **Pfeffer MA and Braunwald E.** Ventricular remodeling after myocardial infarction. Experimental observations and clinical implications. *Circulation* 81: 1161–1172, 1990.
17. **Rosenkranz S.** TGF-β_1 and angiotensin networking in cardiac remodeling. *Cardiovasc Res* 63: 423–432, 2004.
18. **Rosenkranz S, Flesch M, Amann K, Haeuseler C, Kilter H, Seeland U, Schluter KD, and Bohm M.** Alterations of β-adrenergic signaling and cardiac hypertrophy in transgenic mice overexpressing TGF-β_1. *Am J Physiol Heart Circ Physiol* 283: H1253–H1262, 2002.
19. **Sadoshima J and Izumo S.** The cellular and molecular response of cardiac myocytes to mechanical stress. *Annu Rev Physiol* 59: 551–571, 1997.
20. **Sakurai H, Miyoshi H, Toriumi W, and Sugita T.** Functional interactions of transforming growth factor β-activated kinase 1 with IκB kinases to stimulate NF-κB activation. *J Biol Chem* 274: 10641–10648, 1999.
21. **Schnaper HW, Hayashida T, Hubchak SC, and Poncelet AC.** TGF-β signal transduction and mesangial cell fibrogenesis. *Am J Physiol Renal Physiol* 284: F243–F252, 2003.
22. **Schwartz K, Boheler KR, de la Bastie D, Lompre AM, and Mercadier JJ.** Switches in cardiac muscle gene expression as a result of pressure and volume overload. *Am J Physiol Regul Integr Comp Physiol* 262: R364–R369, 1992.
23. **Sutton MG and Sharpe N.** Left ventricular remodeling after myocardial infarction: pathophysiology and therapy. *Circulation* 101: 2981–2988, 2000.
24. **Swynghedauw B.** Molecular mechanisms of myocardial remodeling. *Physiol Rev* 79: 215–262, 1999.
25. **Takahashi N, Calderone A, Izzo NJ Jr, Maki TM, Marsh JD, and Colucci WS.** Hypertrophic stimuli induce transforming growth factor-β_1 expression in rat ventricular myocytes. *J Clin Invest* 94: 1470–1476, 1994.
26. **Takimoto Y, Aoyama T, Tanaka K, Keyamura R, Yui Y, and Sasayama S.** Augmented expression of neuronal nitric oxide synthase in the atria parasympathetically decreases heart rate during acute myocardial infarction in rats. *Circulation* 105: 490–496, 2002.
27. **Thompson NL, Bazoberry F, Speir EH, Casscells W, Ferrans VJ, Flanders KC, Kondaiah P, Geiser AG, and Sporn MB.** Transforming growth factor β-1 in acute myocardial infarction in rats. *Growth Factors* 1: 91–99, 1988.
28. **Wang Y, Huang S, Sah VP, Ross J Jr, Brown JH, Han J, and Chien KR.** Cardiac muscle cell hypertrophy and apoptosis induced by distinct members of the p38 mitogen-activated protein kinase family. *J Biol Chem* 273: 2161–2168, 1998.
29. **Wunsch M, Sharma HS, Markert T, Bernotat-Danielowski S, Schott RJ, Kremer P, Bleese N, and Schaper W.** In situ localization of transforming growth factor β_1 in porcine heart: enhanced expression after chronic coronary artery constriction. *J Mol Cell Cardiol* 23: 1051–1062, 1991.
30. **Yamaguchi K, Shirakabe K, Shibuya H, Irie K, Oishi I, Ueno N, Taniguchi T, Nishida E, and Matsumoto K.** Identification of a member of the MAPKKK family as a potential mediator of TGF-β signal transduction. *Science* 270: 2008–2011, 1995.
31. **Zechner D, Thuerauf DJ, Hanford DS, McDonough PM, and Glembotski CC.** A role for the p38 mitogen-activated protein kinase pathway in myocardial cell growth, sarcomeric organization, and cardiac-specific gene expression. *J Cell Biol* 139: 115–127, 1997.
32. **Zhang D, Gaussin V, Taffet GE, Belaguli NS, Yamada M, Schwartz RJ, Michael LH, Overbeek PA, and Schneider MD.** TAK1 is activated in the myocardium after pressure overload and is sufficient to provoke heart failure in transgenic mice. *Nat Med* 6: 556–563, 2000.

Original Paper

nephron Clinical Practice

Nephron Clin Pract 2006;102:c35–c42
DOI: 10.1159/000088313

Received: February 11, 2005
Accepted: May 30, 2005
Published online: September 19, 2005

Clinical Efficacy of Intravenous Immunoglobulin for Patients with MPO-ANCA-Associated Rapidly Progressive Glomerulonephritis

Toshiko Ito-Ihara[a] Takahiko Ono[a] Fumiaki Nogaki[a] Katsuo Suyama[a]
Mari Tanaka[b] Satomi Yonemoto[b] Atsushi Fukatsu[a] Toru Kita[a]
Kazuo Suzuki[c] Eri Muso[b]

[a]Department of Nephrology and Cardiovascular Medicine, Graduate School of Medicine, Kyoto University, Kyoto, [b]Division of Nephrology, Kitano Hospital, Tazuke Kofukai Foundation, Medical Research Institute, Osaka, and [c]Biodefense Laboratory, National Institute of Infectious Diseases (NIID-NIH), Tokyo, Japan

Key Words
Intravenous immunoglobulin · MPO-ANCA · Tumor necrosis factor-α

Abstract
Background: To determine whether intravenous immunoglobulin (IVIg) can control disease activity in patients with myeloperoxidase-antineutrophil cytoplasmic antibody (MPO-ANCA)-associated rapidly progressive glomerulonephritis (RPGN). ***Methods:*** Twelve patients with serologically and histologically confirmed MPO-ANCA-associated RPGN (7 men, 5 women; mean age 71 ± 3 years) received IVIg (400 mg/kg/day) alone for 5 days. The effects of IVIg were evaluated by white blood cell counts, serum C-reactive protein levels, Birmingham Vasculitis Activity Score, rate of change in reciprocal creatinine (1/Cre), and plasma tumor necrosis factor-α levels after IVIg administration. Corticosteroids with or without cyclophosphamide were commenced after IVIg. ***Results:*** After IVIg treatment, a significant decrease was observed in white blood cell count ($p < 0.05$), C-reactive protein values ($p < 0.001$), and Birmingham Vasculitis Activity Score ($p < 0.001$) concomitant with the amelioration of systemic symptoms. The rate of change in 1/Cre significantly improved ($p < 0.05$). Plasma tumor necrosis factor-α levels that were significantly elevated in patients before IVIg compared with normal controls ($p < 0.0001$), rapidly declined after IVIg with a significant reduction ($p < 0.05$). Three months post-treatment with IVIg, all patients showed improvement of disease without serious infectious complications. ***Conclusion:*** IVIg is a potential component of remission induction therapy for patients with MPO-ANCA-associated RPGN.

Introduction

Antineutrophil cytoplasmic antibody (ANCA)-associated rapidly progressive glomerulonephritis (RPGN), which occurs in Wegener's granulomatosis (WG) and microscopic polyangiitis (MPA) [1], leads to renal failure through systemic vasculitis and diffuse crescentic glomerulonephritis. Since crescent formation has features of delayed-type hypersensitivity and is accompanied by the presence of T cells, macrophages, and fibrin in the glomerular lesion [2], high-dose corticosteroids and cyclophosphamide (CYC) are standard treatment for ANCA-associated RPGN; however, such immunosuppressive therapy is often complicated by severe infection in elderly patients [3]. Therefore, to induce early remission of

KARGER
Fax +41 61 306 12 34
E-Mail karger@karger.ch
www.karger.com

Accessible online at:
www.karger.com/ncc

Eri Muso, MD, PhD
Division of Nephrology, Kitano Hospital
Tazuke Kofukai Foundation, Medical Research Institute
2-4-20, Ohgimachi, Kita-ku, Osaka 530-8480 (Japan)
Tel. +81 6 6312 8824, Fax +81 6 6312 8807, E-Mail muso@kitano-hp.or.jp

the disease including renal insufficiency and to avoid fatal side effects, it is important to establish a therapeutic regimen that can maintain the immune potency of such patients.

Intravenous immunoglobulin (IVIg) has been advocated as a safe and effective treatment for other immune-mediated diseases, such as Kawasaki disease, idiopathic thrombocytopenic purpura, Guillain-Barré syndrome, and chronic inflammatory demyelinating polyneuropathy. European investigators have recently shown that IVIg is clinically useful and safe when administered in conjunction with immunosuppressive drugs, helps suppress disease activity for at least 1 year, and consequently reduces the total dose of immunosuppressive agents in patients with ANCA-associated vasculitis, mainly WG with or without RPGN [4, 5]. Accumulating evidence suggests that it works in multiple phases of immune response; neutralization of circulating pathogenic antibodies, Fc receptor modulation and blockade, or suppression of antibody-dependent cellular toxicity, natural killer cell function, autoantibody production, and complement activation [6]. In addition, Guillain-Barré syndrome patients who received IVIg showed clinical recovery in parallel with reduction in serum levels of tumor necrosis factor-alpha (TNF-α), suggesting an important role of IVIg in inhibiting cytokine activity [7].

Here we report a study evaluating the effectiveness of IVIg as an initial treatment, preceding corticosteroids with or without CYC, in 12 patients with MPO-ANCA-associated RPGN. Since it remains unclear whether IVIg is independently effective [8], we investigated the potential immunomodulatory effect unique to IVIg by comparing renal function, clinical score (Birmingham Vasculitis Activity Score, BVAS), and circulating TNF-α levels before and after IVIg treatment. Since MPO-ANCA-associated RPGN is more common than those related to PR3-ANCA in Asia, which clearly contrasts with the incidence in Western countries, we were able to recruit sufficient numbers of patients with MPO-ANCA-associated RPGN to examine the results statistically. This is the first report of the effects of IVIg in MPO-ANCA-specific RPGN patients.

Patients and Methods

Patients

Twelve consecutive patients with MPO-ANCA-associated RPGN (7 men and 5 women; mean age 72 years; range 57–83 years), who were admitted to the Nephrology Department of Kyoto University Hospital and Kitano Hospital between January 2001 and February 2003, were enrolled in this study (table 1). All patients were diagnosed as having MPA because of elevated serum MPO-ANCA as well as characteristic pathology observed in the renal biopsy specimen before treatment. In all patients, the disease was confirmed based on the definition of MPA described by the Chapel Hill Consensus Conference [9]. Renal involvement was seen in all patients. Patient with rapid aggravation of renal dysfunction with more than 30% rise in serum creatinine (Cre) levels were defined as having RPGN. All except 1 (patient No. 2) were newly diagnosed patients who had been transferred from other hospitals due to the onset of RPGN. Patient 2 had previously demonstrated MPO-ANCA-associated RPGN and recovered after 6 years of treatment with prednisolone and CYC. He again developed fever, arthralgia, and myalgia with elevation of white blood cells (WBC), C-reactive protein (CRP), Cre (33% rise) and MPO-ANCA levels, leading to a diagnosis of MPA recurrence. All patients provided written informed consent for renal biopsy as well as treatment according to the protocol. The hospital Ethical Committee approved the study design.

Histological Evaluation

All renal biopsy specimens showed MPA. Hematoxylin and eosin, periodic acid-Schiff, periodic acid silver-methenamine, Masson trichrome, and elastica van Gieson stain were performed. Direct immunofluorescence studies were performed using frozen sections of renal tissue. Histological activity was assessed as follows: active crescent formation (%) = number of glomeruli with cellular and fibrocellular crescent formation/number of glomeruli without global sclerosis × 100. Each biopsy specimen was scored by two pathologists independently. If there was disagreement between the scores, patients were re-examined by the team to determine a final diagnosis by consensus.

Treatment Protocols

After serum MPO-ANCA, WBC, CRP, renal biopsy, and BVAS were all evaluated to establish a definite diagnosis and activity grading, IVIg was administered intravenously as an initial treatment for 5 consecutive days (400 mg/kg/day). Patients 1–10 received freeze-dried sulfonated human normal immunoglobulin (Kenketsu Venilon-I, Teijin Co., Ltd, Tokyo, Japan), and patients 11 and 12 received freeze-dried polyethylene glycol-treated human normal immunoglobulin (Kenketsu Glovenin-I, Nihon Pharmaceutical Co., Ltd, Tokyo, Japan). Both preparations were free from IgG aggregations that can form in prepared solutions containing sucrose. During IVIg treatment, none of the patients received any other immunosuppressive agents, any blood transfusions, or any intravascular volume repletion treatment. Following the post-IVIg treatment evaluation of clinical scores and laboratory data, all patients received immunosuppressive treatment with oral corticosteroids with or without CYC (table 2). Oral corticosteroids (prednisolone 0–1.0 mg/kg/day) were administered dependent on disease severity and patient age. Methylprednisolone pulse and oral CYC (25–50 mg/day) were also administered to 3 of 12 and 8 of 12 patients, respectively.

Assessment of Disease Activity

Complete blood count and serum markers such as CRP, Cre, and MPO-ANCA were evaluated at the onset of disease, before, and immediately after (mean 6.3 days, range 0–17 days) IVIg, and 1 and 3 months after IVIg. Disease activity was assessed by BVAS before and immediately after IVIg and 1 and 3 months after IVIg. BVAS consists of 59 predefined items derived from clinical, radio-

Table 1. Characteristics of the 12 patients (M/F = 7/5)

Patient	Age	Sex	Data before treatment								
			WBC/μl	CRP mg/l	Cre μmol/l	MPO-ANCA, EU	Active crescents, %	BVAS	extrarenal manifestations	pulmonary involvement	latent and antibiotics resistant infections
1	82	F	7,000	80	283	239	81	19	S, F, E		HBV carrier
2	75	M	9,600	178	106	435	0	23	S, F, A, C, N		MAC, *K. pneumoniae*
3	61	F	8,100	43	126	244	71	15	S, F		
4	82	M	9,400	104	417	159	71	14	S, A		
5	64	F	12,100	154	737	276	81	19	S, F, L	infiltrate	
6	59	M	10,200	139	389	140	90	15	S, F		*Aspergillus*
7	83	F	4,700	1	258	617	60	20	S, F, Ab		
8	82	F	14,700	113	210	306	38	21	S, F, N		
9	57	M	10,700	99	357	980	64	19	S, A, N		
10	62	M	10,100	101	732	370	80	25	S, L, N	nodules	
11	75	M	9,300	60	1,012	82	33	27	S, E, L	infiltrate	HBV carrier, MRSA, *P. aeruginosa*
12	67	M	11,900	68	401	1,740	78	19	S, L	hemoptysis	MRSA
Mean	71		9,820	95	419	466	62	20			
Reference range			3,500–9,100	<3	<106	<20		0			

WBC = White blood cell count; CRP = C-reactive protein; Cre = serum creatinine; MPO-ANCA = myeloperoxidase antineutrophil antibody; BVAS = Birmingham Vasculitis Activity Score; S = systemic symptom (malaise, myalgia, weight loss); F = fever; A = arthralgia; C = cutaneous; E = ear-nose-throat; L = lung; Ab = abdomen; K = kidney; N = neuropathy; HBV = hepatitis B virus; MAC = *Mycobacterium avium* complex; *K. pneumoniae* = *Klebsiella pneumoniae*; MRSA = methicillin-resistant *Staphylococcus aureus; P. aeruginosa* = *Pseudomonas aeruginosa*.

Table 2. Treatment and outcomes after IVIg treatment

Patient	Initial immunosuppressive treatment just after IVIg				Treatment after 3 months			
	mPSL pulse	PSL dosage mg/kg/day	CYC dosage mg/kg/day	dialysis	PSL dosage mg/kg/day	CYC dosage mg/kg/day	dialysis	Cre μmol/l
1	–	0.3	0.7	–	0.3	0	–	124
2	–	0.7	0.4	–	0.3	0.4	–	88
3	–	1.0	1.0	–	0.5	1.1	–	92
4	–	0.5	–	HD	0.7	–	–[1]	308
5	–	1.0	1.0	–	0.6	1.1	–	204
6	1 g, 3 days	0.7	0.8	–	0.3	0	–	177
7	–	0.5	1.3	–	0.3	0	–	203
8	–	0.6	–	–	0.4	–	–	87
9	1 g, 3 days	0.7	0.7	–	0.2	1.7	–	141
10	–	0.8	0.8	–	0.4	0.8	–	353
11	–	0	–	HD	0.5	–	HD	723[2]
12	0.5 g, 3 days	0.5	–	–	0.5	–	–	131
Mean		0.6	0.8[3]		0.4	0.6[3]		173[4]

mPSL pulse = Methylprednisolone pulse therapy; PSL = prednisolone; CYC = cyclophosphamide; Cre = serum creatinine; HD = hemodialysis.

[1] Cessation of HD; [2] Cre level before a hemodialysis; [3] mean CYC dose of 8 patients; [4] patient 11 was excluded.

logic, and laboratory evaluations in 9 organs systems. Each organ system carries a weight (ranging from 0 to 12), and an item is positively scored if the investigator considers it present and caused by active vasculitis. The maximal score is 63 with higher scores indicating more active disease [10].

Evaluation of the Progression Rate of Renal Dysfunction: Rate of Change in 1/Cre

To determine whether rapid progression of renal failure was occurring in these patients, the rate of change in reciprocal Cre (1/Cre) levels (dl/mg/day) was compared before and after IVIg treatment [11]. Briefly, Cre levels (mg/dl) were evaluated at five time points as follows: the first visit to the primary care physician with initial symptoms (Cre1 at time 1 [T1]), admission to the hospital (Cre2 at time 2 [T2]), transfer to the nephrology unit (Cre3 at time 3 [T3]), just before IVIg treatment (Cre4 at time 4 [T4]), and after IVIg treatment without receiving other immunosuppressive treatment (Cre5 at time 5 [T5]). The unit of time was 1 day. The largest value among (1/Cre4-1/Cre1)/(T4-T1), (1/Cre3-1/Cre1)/(T3-T1), and (1/Cre2-1/Cre1)/(T2-T1) was regarded as a rate of change in 1/Cre before IVIg and compared with (1/Cre5-1/Cre4)/(T5-T4). Only patient 11 was excluded from this evaluation because he was already undergoing permanent hemodialysis before IVIg because of rapidly deteriorating renal function.

Measurement of Plasma Cytokines

Venous blood samples were drawn from patients before and after IVIg, and before initiating immunosuppressive therapy. Plasma samples were stored at -80°C until use. Plasma samples were available for 9 patients, in whom cytokine levels were compared before and after IVIg. According to the manufacturer's instructions, the following cytokines were measured: TNF-α, interleukin (IL)-6, IL-8, IL-1β using Human Cytokine UltraSensitive ELISA kit (Biosource International, Camarillo, Calif., USA). Absolute values of these cytokines were also measured using the blood samples from 12 normal controls, and compared with those of the 9 patients. An average of +2 standard deviations (SD) for each cytokine level in the 12 normal controls was considered the upper limit of the normal range.

Statistical Analysis

The significance of differences between pre- and post-IVIg values of clinical laboratory data was assessed by paired Student's t test using StatView II software (version 5.0 for Macintosh; SAS Institute Inc., Cary, N.C., USA). To compare the cytokine levels of normal controls to the pre-IVIg cytokine levels of patients, unpaired t test was used. Fischer's exact test was performed to compare BVAS and laboratory data before IVIg with those after 1 and 3 months. A p value <0.05 was considered significant. All data were expressed as mean ± SEM.

Results

Clinical and Pathological Features before IVIg Treatment

Demographic and clinical characteristics and renal histological findings of 12 patients enrolled in this study are summarized in table 1. All patients were clinically diagnosed as having RPGN with micro- or macroscopic hematuria and rapidly worsening renal function. The mean Cre value was 419 μmol/l (range 106–1,012) just before IVIg treatment. The mean BVAS was 20 (range 14–27) before treatment. Laboratory tests demonstrated increased levels of WBC (mean 9,820/μl; range 4,700–14,700), CRP (mean 90 mg/l; range 1.0–178; reference <3), and MPO-ANCA level (mean 466 EU; range 82–1,740; reference <20). Crescentic glomerulonephritis with or without systemic features of MPA was present in all patients. Mean percentage of active crescent formation was 62%. Direct immunofluorescence study demonstrated pauci-immune deposition (scant depositions of immunoglobulins) in all patients.

Clinical Responses

(1) The change in WBC count and CRP value: Total WBC counts were 9,820 ± 740/μl before IVIg and decreased to 7,960 ± 870/μl after IVIg; the pre- and post-treatment levels were significantly different ($p < 0.01$). A significant decrease was also observed in neutrophil, lymphocyte, and eosinophil differential counts: the decrease in neutrophils was the most significant (pre-IVIg 7,950 ± 740/μl; post-IVIg 6,010 ± 800; $p < 0.001$). Mean CRP value was 97 mg/l (range 5–178) at the onset of vasculitis, and 95 mg/l (range 1–178) just before IVIg treatment. Following IVIg, the mean CRP value decreased significantly to 57 mg/l (range 1–124) ($p < 0.001$; fig. 1a).

(2) Rapid effect on renal function: The mean Cre level was 89 μmol/l (range 44–124) at the onset of disease, but increased to 365 μmol/l (range 106–737) in 62 ± 14 days (range 22–185) just before IVIg (fig. 1b). As a sensitive method of detecting rapid changes in renal dysfunction, we calculated the rate of change in 1/Cre before and after IVIg as shown previously [11]. The rate of change in 1/Cre was -0.041 ± 0.020 dl/mg/day before IVIg and increased to 0.007 ± 0.004 dl/mg/day after IVIg ($p < 0.05$).

(3) Temporal profiles of pro-inflammatory cytokine levels before and after IVIg: Before IVIg treatment, the plasma TNF-α levels were significantly elevated in patients compared to normal controls (patients, pre-IVIg 4.23 ± 0.92 pg/ml vs. control, 0.23 ± 0.40 pg/ml; $p < 0.0001$). After IVIg treatment, the plasma TNF-α levels decreased significantly (pre-IVIg 4.23 ± 0.92 pg/ml vs. post-IVIg 2.40 ± 0.53; $p < 0.05$; fig. 2). Plasma IL-6 levels (pg/ml) were significantly higher before IVIg treatment in patients compared to that in normal controls (pre-IVIg 2.75 ± 4.45 vs. control, 0.00 ± 0.00; $p < 0.05$). The plasma IL-6 levels decreased on average after IVIg treatment, but the difference did not reach significance (data not shown).

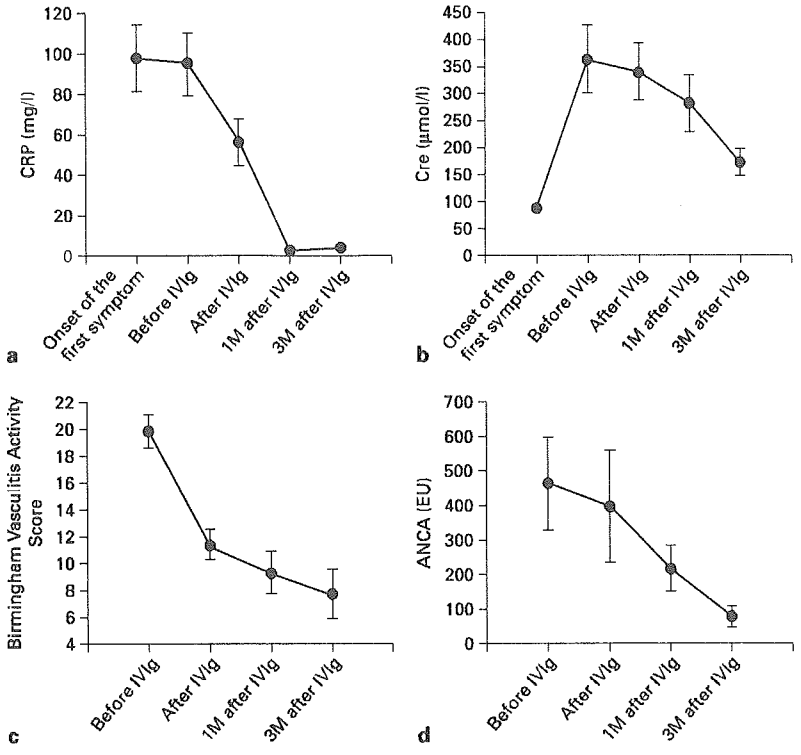

Fig. 1. Three-month follow-up of the patients. **a** Serum C-reactive protein (CRP), mg/l (n = 12). **b** Serum creatinine (Cre) level, μmol/l (n = 11). **c** Birmingham Vasculitis Activity Score (n = 12). **d** Anti-neutrophil cytoplasmic antibody (ANCA) (n = 12). M = Months.

The plasma IL-8 levels of patients before IVIg treatment did not significantly differ from that of normal controls or that after IVIg treatment (data not shown). Some patients showed markedly elevated IL-6 (patient No. 1, 6, 8–10) and IL-8 (patient No. 1, 5, 8–10) levels before IVIg treatment, which decreased after IVIg treatment. The plasma IL-1β levels (pg/ml) of patients before IVIg treatment did not significantly differ from that of normal controls or that after IVIg treatment (data not shown).

(4) BVAS: After IVIg treatment, significant reduction was seen in BVAS (pre-IVIg 20 ± 1; post-IVIg 11 ± 1; $p < 0.0001$; fig. 1c). First, systemic symptoms improved: malaise (8 of 12), myalgia (3 of 3), arthralgia/arthritis (2 of 2), and fever (7 of 9). Before IVIg treatment, hematuria and proteinuria were observed in all patients; rapid aggravation of renal dysfunction with more than 30% rise in Cre was also noted in all patients. Lung involvement was seen in 4 patients; 1 showed nodular lesions, 1 showed hemoptysis and the other 2 showed infiltrative lesions. These lesions improved partially following IVIg.

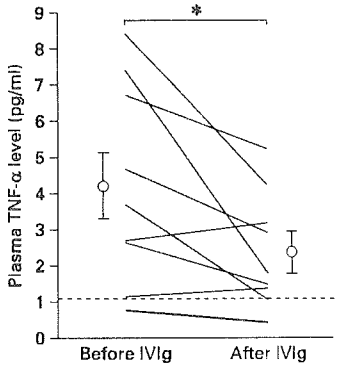

Fig. 2. Plasma TNF-α levels (pg/ml) before and after IVIg (n = 9). The dotted line represents the upper limit of the normal range. * $p < 0.05$ vs. before IVIg.

Immunosuppressive Therapy following IVIg Therapy

Following the 5-day IVIg course, 12 patients were treated as summarized in table 2. After IVIg, 3 patients received steroid pulse treatment and 11 patients received oral steroids with no more than 1.0 mg/kg/day, 6.3 days after IVIg treatment on average (range 0–17). The mean initial dose of oral steroid for 12 patients was 0.6 ± 0.1 mg/kg/day (33.3 ± 4.5 mg/day). Additionally, those who responded inadequately to steroids received CYC unless active infections were concurrent. CYC was administered to 8 patients at a mean dose of 0.8 ± 0.1 mg/kg/day (46.9 ± 3.1 mg/day).

Outcome and 3-Month Follow-Up

There were no disease-related deaths for 3 months after IVIg treatment. Vasculitis recurred 3 months after IVIg treatment in patient 11 who did not receive any immunosuppressive drugs after IVIg treatment because he was a carrier of MRSA and antibiotic-resistant *Pseudomonas aeruginosa*. There was no fatal complication due to infections in any of the patients during the 3-month observation period after treatment.

CRP level continued to decrease and normalized 3 months after IVIg treatment (4.0 ± 2.0 mg/l; $p < 0.0001$ vs. before IVIg; fig. 1a).

As shown in figure 1b, the Cre level began to decrease following IVIg; Cre level was 173 μmol/l (range 88–353; except for patient 11 who was on maintenance hemodialysis) 3 months after IVIg treatment (vs. pre-IVIg; $p < 0.0001$). Among 3 patients (patient No. 5, 10, and 11) whose Cre level exceeded 700 μmol/l before IVIg treatment, only one patient (No. 11) required chronic hemodialysis within 3 months after IVIg treatment. Although hemodialysis was also required for patient 4 within 1 month after IVIg treatment, he could be withdrawn from hemodialysis shortly thereafter. Collectively, the 3-month renal survival rate was 92% in our 12 patients.

The mean BVAS continued to decrease after IVIg treatment (fig. 1c). The mean BVAS was 20 (range 15–27) before IVIg and 11 (range 1–16) immediately after IVIg ($p < 0.0001$); 9 (range 0–19) 1 month after IVIg ($p < 0.0001$ vs. pre-IVIg BVAS), and 8 (range 0–22) 3 months after IVIg ($p < 0.0001$ vs. pre-IVIg BVAS). In particular, urinalysis showed that hematuria and/or proteinuria disappeared in 8 patients, 3 months after IVIg treatment. Systemic symptoms such as body weight loss, and nervous or alimentary tract symptoms also improved at 3 months after IVIg treatment.

The mean MPO-ANCA levels obtained within 8 ± 5 days after IVIg treatment were 401 EU (range 70–990) and those 1 month after IVIg treatment were 218 EU (range 13–640). The titers at these two time points after IVIg treatment were not significantly different from that prior to IVIg treatment (465.7 ± 135.7 EU). The mean MPO-ANCA levels 3 months after IVIg treatment, 78.8 EU (range 0–389), were significantly lower than that prior to IVIg treatment ($p < 0.01$; fig. 1d).

Adverse Drug Reaction

There were no major side effects observed in patients who received IVIg treatment. Patient 4 experienced transient mild hypertension and edema of the extremities during IVIg infusion, but it subsided when the rate of infusion of IVIg was lowered.

Discussion

The present study was conducted to evaluate the safety and efficacy of IVIg as an initial therapy for patients with MPO-ANCA-associated RPGN. All 12 patients with ANCA-associated RPGN enrolled in this study had experienced rapidly deteriorating renal dysfunction with multiorgan involvement. Administration of IVIg for 5 consecutive days led to partial resolution of inflammatory signs and symptoms in parallel with significant decreases in CRP, TNF-α, and BVAS values as well as cessation of progression in renal dysfunction. No life-threatening infections or side effects developed with our regimens including IVIg in all patients, including those older than 80 (patient No. 1, 4, 7, 8) and those with latent, antibiotic-resistant infections (patient No. 1, 2, 6, 11, 12). Clinical improvement was seen in all patients with IVIg for initial therapy followed by immunosuppressants, none of whom died within 3 months. The 3-month renal and patient survival rates were 92 and 100%, respectively, which were more favorable than those previously reported in MPO-ANCA-positive RPGN patients treated with immunosuppressive agents in Japan: 3-month renal and patient survival rates were about 75 and 85%, respectively [12].

Notably, there was a rapid and significant decrease in neutrophil count following IVIg treatment. Activated neutrophils are known to be involved in vasculitis. During the active phase of Kawasaki disease, circulating activated neutrophils increase in number and secrete excessive amounts of autotoxic mediators such as reactive oxygen species and elastase. In this active phase, neutrophil apoptosis is inhibited, resulting in a prolonged lifespan, which then might contribute to the pathogenesis of the

vasculitic lesions. High-dose IVIg therapy decreased the number of circulating neutrophils by accelerating their apoptosis in Kawasaki disease and was effective in preventing the development of coronary aneurysm [13]. Similarly, in MPO-ANCA-associated vasculitis, activated neutrophils are involved in renal damage. TNF-α-primed neutrophils undergo accelerated and dysregulated apoptosis, and such apoptotic neutrophils express ANCA antigen on their cell surface in affected organs, where leukocytoclasia can further augment inflammatory injury [14]. Although the precise mechanism by which IVIg affects the apoptosis of neutrophils remains unknown, the rapid decrease of WBC count following IVIg treatment coupled with the significant decrease in CRP suggests accelerated clearance of apoptotic neutrophils by IVIg in patients with MPO-ANCA-associated RPGN in this study.

Our study showed that the plasma TNF-α value significantly decreased following IVIg treatment, suggesting immunomodulatory effect of IVIg. Serum levels of TNF-α were reported to be increased in patients with active vasculitis [15]. In addition, elevation of serum TNF-α was associated with upregulation of TNF-α mRNA at the sites of vasculitis [16]. TNF-α released from activated macrophages following infectious stimuli is known to prime and activate neutrophils. Once activated, neutrophils can attach to the endothelium and further release MPO and reactive oxygen species, ultimately leading to endothelial damage [17, 18]. Consistent with this, Booth et al. [19] recently reported TNF-α blockade with infliximab was effective at inducing remission in 88% of patients with ANCA vasculitis. Their report and our findings suggest that TNF-α may play a key role in ANCA-associated vasculitis. Decrease in the TNF-α value following IVIg suggests that IVIg plays a positive role in disrupting such a vicious inflammatory cycle.

Another possible mechanism of IVIg is that therapeutic concentrations of IgG block Fc receptors on phagocytes and inhibit antibody-dependent cell-mediated cytotoxicity [6] or downregulate the proliferation of activated B and T cells, reducing cytokine production from these immunoeffector cells [20]. Because the latter mechanism requires a substantial time interval, the rapid TNF-α suppression with IVIg observed in this study suggests that IVIg has direct effects on activated macrophages, rather than an effect mediated through T- or B-cell suppression.

IVIg treatment, even without immunosuppressants, has been shown to ameliorate systemic symptoms of active vasculitis [8]. In patients with asthma, IVIg was found to act synergistically with steroids, improved the clinical parameters, and reduced oral corticosteroid requirements and the duration of hospitalization. Such effects are partially mediated by improvement in glucocorticoid-receptor-binding affinity [21]. In the present study, RPGN was significantly improved by a relatively low initial dose of steroid (0.6 mg/kg/day). Our patients, who are relatively old and therefore at higher risk of developing infectious complications after steroid administration, might have benefited from the potential steroid-sparing effect of IVIg.

A major side effect of IVIg is renal dysfunction probably due to hyperosmolarity induced by sucrose contained in immunoglobulin formulations [22]. Therefore, in Europe, such a formulation is used for WG patients without renal involvement, but not for those with renal involvement. For MPA patients with renal involvement, we used immunoglobulin formulation that contained mannitol (Kenketsu Venilon-I) or glucose (Kenketsu Glovenin-I) instead of sucrose because the former two substances are less likely to cause hyperosmolarity. Although we cannot exclude the possibility that intravascular volume repletion with mannitol might have increased tubular flow, there is no convincing evidence for the efficacy of mannitol in RPGN [23]. With our regimen, patients demonstrated improved renal function, supporting the safety of IVIg with mannitol or glucose.

In conclusion, the present study demonstrated the safety and potential efficacy of IVIg as an initial therapy for patients with MPO-ANCA-associated RPGN. Our study is limited by its small size, relatively few severe cases, and non-standardized follow-up protocols. However, our findings suggest that IVIg is potentially effective for treating MPO-ANCA-associated RPGN, either as first-line or adjunctive therapy. Further research into the optimal dose and duration of treatment is required to define the role of IVIg in treatment of MPO-ANCA-associated RPGN.

Acknowledgments

We wish to thank Drs. Ning Liu, Noriyuki Iehara, Hidenori Arai, and Masafumi Ihara for excellent advice. This work was supported by a Research Grant on Pharmaceutical and Medical Safety, Ministry of Health, Labour, and Welfare, through NIID-NIH, Japan.

References

1 Van der Woude FJ, Rasmussen N, Lobatto S, Wiik A, Permin H, van Es LA, van der Giessen M, van der Hem GK, The TH: Autoantibodies against neutrophils and monocytes: tool for diagnosis and marker of disease activity in Wegener's granulomatosis. Lancet 1985;i:425–429.

2 Cunningham MA, Ono T, Hewitson TD, Tipping PG, Becker GJ, Holdsworth SR: Tissue factor pathway inhibitor expression in human crescentic glomerulonephritis. Kidney Int 1999;55:1311–1318.

3 Harper L, Savage CO: ANCA-associated renal vasculitis at the end of the twentieth century – a disease of older patients. Rheumatology (Oxford) 2005;44:495–501.

4 Jayne DR, Davies MJ, Fox CJ, Black CM, Lockwood CM: Treatment of systemic vasculitis with pooled intravenous immunoglobulin. Lancet 1991;337:1137–1139.

5 Jayne DR, Chapel H, Adu D, Misbah S, O'Donoghue D, Scott D, Lockwood CM: Intravenous immunoglobulin for ANCA-associated systemic vasculitis with persistent disease activity. QJM 2000;93:433–439.

6 Kazatchkine MD, Kaveri SV: Immunomodulation of autoimmune and inflammatory diseases with intravenous immune globulin. N Engl J Med 2001;345:747–755.

7 Sharief MK, Ingram DA, Swash M, Thompson EJ: Intravenous immunoglobulin reduces circulating proinflammatory cytokines in Guillain-Barré syndrome. Neurology 1999;52:1833–1838.

8 Jayne DR, Lockwood CM: Intravenous immunoglobulin as sole therapy for systemic vasculitis. Br J Rheumatol 1996;35:1150–1153.

9 Jennette JC, Falk RJ, Andrassy K, Bacon PA, Churg J, Gross WL, Hagen EC, Hoffman GS, Hunder GG, Kallenberg CG, et al: Nomenclature of systemic vasculitides. Proposal of an international consensus conference. Arthritis Rheum 1994;37:187–192.

10 Luqmani RA, Bacon PA, Moots RJ, Janssen BA, Pall A, Emery P, Savage C, Adu D: Birmingham Vasculitis Activity Score (BVAS) in systemic necrotizing vasculitis. QJM 1994;87:671–678.

11 Yashiro M, Muso E, Itoh-Ihara T, Oyama A, Hashimoto K, Kawamura T, Ono T, Sasayama S: Significantly high regional morbidity of MPO-ANCA-related angiitis and/or nephritis with respiratory tract involvement after the 1995 great earthquake in Kobe (Japan). Am J Kidney Dis 2000;35:889–895.

12 Sakai H, Kurokawa K, Koyama A, Shiiki H, Nishi S, Mitarai T, Yokoyama H, Yoshimura A, Yorioka N: Guidelines for the management of rapidly progressive glomerulonephritis. Nippon Jinzo Gakkai Shi 2002;44:55–82.

13 Tsujimoto H, Takeshita S, Nakatani K, Kawamura Y, Tokutomi T, Sekine I: Intravenous immunoglobulin therapy induces neutrophil apoptosis in Kawasaki disease. Clin Immunol 2002;103:161–168.

14 Harper L, Ren Y, Savill J, Adu D, Savage CO: Antineutrophil cytoplasmic antibodies induce reactive oxygen-dependent dysregulation of primed neutrophil apoptosis and clearance by macrophages. Am J Pathol 2000;157:211–220.

15 Arimura Y, Minoshima S, Kamiya Y, Tanaka U, Nakabayashi K, Kitamoto K, Nagasawa T, Sasaki T, Suzuki K: Serum myeloperoxidase and serum cytokines in anti-myeloperoxidase antibody-associated glomerulonephritis. Clin Nephrol 1993;40:256–264.

16 Noronha IL, Kruger C, Andrassy K, Ritz E, Waldherr R: In situ production of TNF-α, IL-1β and IL-2R in ANCA-positive glomerulonephritis. Kidney Int 1993;43:682–692.

17 Falk RJ, Terrell RS, Charles LA, Jennette JC: Anti-neutrophil cytoplasmic autoantibodies induce neutrophils to degranulate and produce oxygen radicals in vitro. Proc Natl Acad Sci USA 1990;87:4115–4119.

18 Savage CO, Pottinger BE, Gaskin G, Pusey CD, Pearson JD: Autoantibodies developing to myeloperoxidase and proteinase 3 in systemic vasculitis stimulate neutrophil cytotoxicity toward cultured endothelial cells. Am J Pathol 1992;141:335–342.

19 Booth A, Harper L, Hammad T, Bacon P, Griffith M, Levy J, Savage C, Pusey C, Jayne D: Prospective study of TNF-α blockade with infliximab in anti-neutrophil cytoplasmic antibody-associated systemic vasculitis. J Am Soc Nephrol 2004;15:717–721.

20 Kaveri S, Vassilev T, Hurez V, Lengagne R, Lefranc C, Cot S, Pouletty P, Glotz D, Kazatchkine MD: Antibodies to a conserved region of HLA class I molecules, capable of modulating CD8 T cell-mediated function, are present in pooled normal immunoglobulin for therapeutic use. J Clin Invest 1996;97:865–869.

21 Spahn JD, Leung DY, Chan MT, Szefler SJ, Gelfand EW: Mechanisms of glucocorticoid reduction in asthmatic subjects treated with intravenous immunoglobulin. J Allergy Clin Immunol 1999;103:421–426.

22 Cayco AV, Perazella MA, Hayslett JP: Renal insufficiency after intravenous immune globulin therapy: a report of two cases and an analysis of the literature. J Am Soc Nephrol 1997;8:1788–1794.

23 Girbes AR: Prevention of acute renal failure: role of vasoactive drugs, mannitol and diuretics. Int J Artif Organs 2004;27:1049–1053.

Plasma ghrelin levels in healthy elderly volunteers: the levels of acylated ghrelin in elderly females correlate positively with serum IGF-I levels and bowel movement frequency and negatively with systolic blood pressure

T Akamizu[1], T Murayama[4], S Teramukai[3], K Miura[2], I Bando[4], T Irako[1], H Iwakura[1], H Ariyasu[1], H Hosoda[1,8], H Tada[3], A Matsuyama[3], S Kojima[3], T Wada[5], Y Wakatsuki[5], K Matsubayashi[6], T Kawakita[7], A Shimizu[2], M Fukushima[3], M Yokode[3] and K Kangawa[1,8]

[1]Ghrelin Research Project and [2]Post-genome Project, Department of Experimental Therapeutics, Kyoto University Hospital, 54 Shogoin-kawaharacho, Sakyo-ku, Kyoto 606-8507, Japan

[3]Department of Clinical Innovative Medicine, and [4]Department of Clinical Trial Design and Management, Kyoto University Hospital, Kyoto 606-8507, Japan

[5]Translational Research Center, Kyoto University Hospital, and Department of Geriatric Medicine, Kyoto University School of Medicine, Kyoto 606-8507, Japan

[6]Center for Southeast Asian Studies, Kyoto University, Kyoto 606-8501, Japan

[7]Kyoto Preventive Medical Centre, Kyoto 604-8491, Japan

[8]Department of Biochemistry, National Cardiovascular Center Research Institute, Osaka 565-8565, Japan

(Requests for offprints should be addressed to T Akamizu; Email: akamizu@kuhp.kyoto-u.ac.jp)

Abstract

Aging is associated with a decrease in growth hormone (GH) secretion, appetite and energy intake. As ghrelin stimulates both GH secretion and appetite, reductions in ghrelin levels may be involved in the reductions in GH secretion and appetite observed in the elderly. However, only preliminary studies have been performed on the role of ghrelin in elderly subjects. In this study, we sought to clarify the physiologic implications of the age-related alterations in ghrelin secretion by determining plasma ghrelin levels and other clinical parameters in healthy elderly subjects. Subjects were ≥65 years old, corresponding to the SENIEUR protocol, had not had a resection of the upper gastrointestinal tract and had not been treated with hormones. One hundred and five volunteers (49 men and 56 women) were admitted to this study (73·4 ± 6·3 years old). Plasma levels of acylated ghrelin in elderly female subjects positively correlated with serum IGF-I levels and bowel movement frequency and negatively with systolic blood pressure. In elderly men, desacyl ghrelin levels correlated only weakly with bowel movement frequency. These findings suggest that the plasma levels of the acylated form of ghrelin may influence the age-related alterations in GH/IGF-I regulation, blood pressure and bowel motility. These observational associations warrant further experimental studies to clarify the physiologic significance of these effects.

Journal of Endocrinology (2006) **188,** 333–344

Introduction

Aging is associated with progressive decreases in growth hormone (GH) secretion, appetite and energy intake (Wurtman *et al.* 1988, Corpas *et al.* 1993, Morley 1997, Muller *et al.* 1999). This reduced GH secretion is termed 'somatopause' and may be a cause of age-related metabolic and physiologic changes, including reduced lean body mass and expansion of adipose mass. Altered blood lipid profiles also favor the development of vascular diseases that may increase overall mortality. The age-related reduction in energy intake has been termed 'the anorexia of aging' and predisposes to the development of undernutrition (Morley 1997). Common in older people, undernutrition has been implicated in the development and progression of chronic diseases commonly affecting the elderly, as well as in increasing mortality (Wurtman *et al.* 1988).

The mechanisms underlying the reduced GH secretion in aged animals and humans are complex (Muller *et al.* 1999,

Journal of Endocrinology (2006) **188,** 333–344
0022-0795/06/0188-333
DOI: 10.1677/joe.1.06442
Online version via http://www.endocrinology-journals.org

Chapman 2000). Age-related changes appear to involve the function of hypothalamic peptides specifically regulating GH secretion, and GH-releasing hormone (GHRH) and somatostatin (SS), appear to play a major role in this event. Experimental evidence indicates that within the rat hypothalamus, GHRH synthesis is impaired with increased age; relative hyperfunction of the SS-ergic system is also found in this animal. The physiologic causes of the anorexia of aging are largely unknown and probably multifactorial (Morley 1997). Possible mechanisms include a reduction in the central and/or peripheral feeding drives and increased activity of central and/or peripheral satiety signals (Martinez *et al.* 1993, Morley 1997, de Jong *et al.* 1999).

Ghrelin, a 28-amino-acid peptide, exhibits a variety of actions, including vasorelaxation (Nagaya *et al.* 2001, Shimizu *et al.* 2003) and stimulation of GH secretion (Takaya *et al.* 2000, Arvat *et al.* 2001, Hataya *et al.* 2001), appetite (Korbonits *et al.* 2004, van der Lely *et al.* 2004) and gastrointestinal motility (Masuda *et al.* 2000, Trudel *et al.* 2002, Fujino *et al.* 2003). A portion of ghrelin possesses a unique fatty acid modification, *n*-octanoylation, at Ser 3 (Kojima *et al.* 1999). Of the two circulating forms of ghrelin, acylated and unacylated (desacyl), the acylated form is thought to be essential for ghrelin biologic activity. Recently, however, desacyl ghrelin was reported to influence both cell proliferation and adipogenesis (Cassoni *et al.* 2001, Bedendi *et al.* 2003, Broglio *et al.* 2004, Thompson *et al.* 2004), prompting us to hypothesize that alterations in ghrelin may be involved in the reduction of GH secretion and appetite in elderly subjects. Preliminary studies using small numbers of elderly subjects demonstrated that the mean plasma concentrations of total ghrelin in normal weight geriatric subjects were lower than those present in younger, normal-weight subjects (Rigamonti *et al.* 2002, Sturm *et al.* 2003). In addition, GH response to ghrelin administration in elderly subjects is lower than that seen in young subjects (Broglio *et al.* 2003). While ghrelin mRNA levels in the stomach gradually decrease with increasing age in rats, serum levels of total ghrelin did not exhibit obvious age-related variation (Liu *et al.* 2002). In contrast, studies in rat indicated that both stomach ghrelin secretion and ghrelin-induced GH secretion increased in aged rats in comparison to younger rats (Englander *et al.* 2004). Total ghrelin secretion also increases with aging in monkeys (Angeloni *et al.* 2004). Although the disparity between humans and other animal models may be due to species differences, the number of human subjects was rather small. In addition, no adjustment of plasma ghrelin levels by other parameters was attempted, leaving the results of these human studies in question.

In this study, we determined the plasma concentrations of the two ghrelin forms, acylated and desacyl ghrelin, and their relationship to various anthropometric, hormonal and metabolic parameters in 105 elderly volunteers. Using these measurements and appropriate analyses, we sought to clarify the age-related alteration in ghrelin secretion and the associated physiologic implications in elderly subjects.

Materials and Methods

Subjects

One hundred and thirty-seven (62 male and 75 female) elderly volunteers were registered for our study. Thirty-two that did not satisfy the criteria for this study were excluded. Finally, 105 (49 male and 56 female) volunteers aged 65–94 years were subjected to analysis. All of the subjects were Japanese, and were recruited from the outpatient clinics of Kyoto University Hospital ($n=66$ (male, $n=36$; female, $n=30$)) and Kyoto Preventive Medical Center ($n=39$ (male, $n=13$; female, $n=26$)). The inclusion criteria were as follows: 1. ≥ 65 years of age; 2. correspondence with the SENIEUR protocol (Ligthart *et al.* 1984); 3. provision of written consent to participate in this study. Patients with either past history of upper gastrointestinal tract resection or present use of either hormones or steroids were excluded. The SENIEUR protocol provides strict admission criteria for human immunogerontologic studies. This protocol used clinical information (infection, inflammation, malignancy and other conditions, including acute myocardial infarction, treated cardiac insufficiency, hypertension of arteriosclerotic or diabetic origin, dementia, pregnancy, malnutrition, alcoholism and drug abuse), laboratory data (erythrocyte sedimentation rate, hemoglobin levels, mean corpuscular volume, leukocyte count with differentiation, immunoelectrophoresis, urinalysis and serum concentrations of urea, alkaline phosphatase, glucose, ASAT, ALAT and protein) and pharmacologic interference (prescribed medication for the treatment of the disorders defined above, anti-inflammatory drugs, hormones and analgesics) (Ligthart *et al.* 1984). This study included two exclusion criteria (no past resection of the upper gastrointestinal tract and no current treatment with hormones or steroids) to optimize endocrinologic and metabolic examination of stomach-derived hormones. The subjects who met all criteria were recognized as healthy subjects. Younger subjects, in whom plasma ghrelin levels were used for comparison with those in elderly subjects, were described previously (Akamizu *et al.* 2005). They were 16 male and 20 female Japanese volunteers 21–61 years of age. None of the subjects suffered from any known medical conditions or were currently taking medication. The period of the study was from March to September 2004. The study protocol was approved by the ethics committees on human research of Kyoto University Graduate School of Medicine and Kyoto Preventive Medical Center. Written, informed consent was obtained from all subjects prior to enrollment.

Laboratory analyses and biomedical factors

Blood samples for hormone and glucose analyses were drawn from a forearm vein in the morning after overnight fast. Plasma samples were prepared as previously described (Kojima *et al.* 1999, Akamizu *et al.* 2005). Blood samples were immediately transferred to chilled polypropylene tubes containing EDTA-2Na (1 mg/ml) and aprotinin (Ohkura Pharmaceutical, Kyoto, Japan: 500 kallikrein inactivator U/ml), were centrifuged at 4 °C. We added 1 N mol/l HCl (10% volume of plasma volume) to the separated plasma immediately. Plasma levels of acylated and unacylated ghrelin were measured with two commercially available ELISA kits, the Active Ghrelin ELISA and Desacyl-Ghrelin ELISA respectively, according to the manufacturer's protocol (Mitsubishi Kagaku Iatron, Tokyo, Japan) (Akamizu *et al.* 2005). The minimal detection limits for acylated and desacyl ghrelin in this assay system were 2·5 and 12·5 fmol/ml respectively. The intra- and interassay coefficients of variation were 6·5% and 9·8% for acylated ghrelin and 3·7% and 8·1% for desacyl ghrelin respectively. Ghrelin measurements of samples from the older and young subjects were performed with the same kits, but not in the same assay. Plasma glucose was measured by the glucose oxidase method. Serum GH, insulin-like growth factor (IGF)-I and insulin concentrations were measured by immunoradiometric assay (IRMA), while serum leptin levels were measured by RIA (Mitsubishi Kagaku Bio-Clinical Laboratories, Tokyo, Japan). Insulin resistance was calculated according to the homeostasis model of assessment of insulin resistance (HOMA-IR), calculated as insulin (μU/ml) × blood glucose (mmol/l)/22·5 (Haffner *et al.* 1997).

The questionnaire presented to all subjects collected information about their sleeping time duration, bowel movements, smoking habits, alcohol consumption, use of medication, past medical history and physical activity. The question about bowel frequency was, 'How often do you usually defecate – once a day, more than once a day or once per 2 or 3 days?'

Statistical analysis

Data are expressed as the mean ± S.D. We used Student's *t*-test to compare the means of the variables measured in both groups. The relationships between ghrelin concentrations and the variables studied were assessed by multiple regression analysis. The variables examined in the multiple regression models were site of recruitment, gender, age or age group (elderly and younger group), body-mass index (BMI), sleeping duration and blood levels of GH, IGF-I, insulin, glucose and leptin. The associations between ghrelin concentrations and blood pressure or bowel movement were assessed by multiple regression analysis after adjustment by the potential confounding factors according to gender. As the ghrelin distribution was slightly skewed, natural logarithms of ghrelin were used for the regression analysis. To identify the subsets of parameters that are statistically significantly related to each hormone level, we performed multiple regression analysis with a backward-elimination procedure after adjustment for the potential effect of site. All statistical analyses were performed by SAS, Version 8·02 (SAS Institute, Cary, NC, USA). *P* values less than 0·05 were considered to be statistically significant.

Results

Plasma ghrelin concentrations in elderly subjects

We examined the anthropometric, hormonal and metabolic parameters of elderly volunteers (Table 1). The levels of acylated ghrelin in plasma were not significantly different between male and female subjects, while plasma levels of desacyl ghrelin in female subjects were significantly higher than those observed in male subjects (male, 53·3 ± 41·5 fmol/ml; female, 72·0 ± 46·1 fmol/ml; $P=0·031$). In comparison to our previous study of younger volunteers (mean age = 33·5 ± 9·0, $n=36$) (Akamizu *et al.* 2005), plasma levels of acylated ghrelin in elderly female subjects were significantly reduced from the levels in younger female subjects (11·9 ± 9·8 vs 19·9 ± 9·8 fmol/ml; $P=0·004$) (Fig. 1A and B). We did not observe any significant differences in the plasma levels of acylated ghrelin in men (9·3 ± 11·6 vs 10·9 ± 6·1 fmol/ml) or desacyl ghrelin levels in both sexes (male, 53·3 ± 41·5 vs 49·1 ± 23·5 fmol/ml; female, 72·0 ± 46·1 vs 79·8 ± 53·9 fmol/ml) between the elder and younger subjects. The ratios of acylated to desacyl ghrelin (A/D ratio) in elderly female subjects were significantly lower than those in younger female subjects (16·3 ± 8·2 vs 26·8 ± 7·8; $P=0·001$). Men did not exhibit any significant differences between the age groups (18·0 ± 11·0 vs 22·6 ± 8·8; $P=0·101$) (Fig. 1C). Age, BMI, insulin, leptin and HOMA-IR levels, however, also differed significantly between the sexes. In addition, the volunteers were recruited from two independent sites. Although nearly all of the parameters, including ghrelin levels, did not differ significantly between the sites, the A/D ratios in both sexes and diastolic blood pressure (BP) values in men were significantly different (Table 1). To account for these differences, recruitment site, gender and age group were included as independent variables in the multiple regression analyses.

Correlations of ghrelin concentrations with various parameters in elderly subjects

In contrast to the results in Student's *t*-test, plasma levels of acylated ghrelin in women were not correlated with age group in the multiple regression analyses ($P=0·914$) (Table 2), suggesting that those in elderly female subjects

Table 1 Characteristcs of elderly subjects and their plasma ghrelin concentrations

		Male				Female			
	All (n=105)	All (n=49)	KPMC (n=13)	KUH (n=36)	P value*	All (n=56)	KPMC (n=26)	KUH (n=30)	P value*	P value**
Parameters										
Age (years)	73·4 ± 6·3	75·0 ± 7·0	72·8 ± 4·7	75·8 ± 7·5	0·119	72·0 ± 5·4	69·4 ± 4·7	74·2 ± 5·1	**0·001**	**0·017**
Height (cm)	155·8 ± 8·4	162·1 ± 6·5	163·1 ± 5·1	161·8 ± 6·9	0·488	150·3 ± 5·5	151·3 ± 4·2	149·3 ± 6·4	0·162	**0·001**
Body weight (kg)	55·5 ± 8·5	58·3 ± 9·0	60·4 ± 4·8	57·5 ± 10·0	0·182	53·1 ± 7·2	54·3 ± 7·2	52·1 ± 7·3	0·261	**0·002**
BMI (kg/m^2)	22·9 ± 2·8	22·1 ± 2·6	22·8 ± 1·9	21·9 ± 2·7	0·205	23·5 ± 2·8	23·7 ± 2·9	23·4 ± 2·8	0·671	**0·008**
Acylated ghrelin (fmol/ml)	10·7 ± 10·7	9·3 ± 11·6	6·4 ± 2·8	10·4 ± 13·3	0·099	11·9 ± 9·8	9·8 ± 8·3	13·8 ± 10·8	0·129	0·213
Desacyl ghrelin (fmol/ml)	63·2 ± 44·8	53·3 ± 41·5	65·1 ± 33·6	49·0 ± 43·7	0·183	72·0 ± 46·1	77·3 ± 51·3	67·3 ± 41·4	0·431	**0·031**
A/D ratio (%)	17·1 ± 9·6	18·0 ± 11·0	11·7 ± 6·8	20·3 ± 11·5	**0·003**	16·3 ± 8·2	12·5 ± 5·6	19·6 ± 8·6	**0·001**	0·379
GH (ng/ml)	2·5 ± 3·7	2·5 ± 4·7	3·9 ± 6·7	2·0 ± 3·7	0·349	2·5 ± 2·6	2·8 ± 2·8	2·2 ± 2·4	0·395	0·929
IGF-I (ng/ml)	125·5 ± 36·8	128·5 ± 41·1	134·9 ± 20·8	126·2 ± 46·3	0·370	122·8 ± 32·7	121·7 ± 28·5	123·8 ± 36·5	0·813	0·440
Insulin (μU/ml)	6·1 ± 4·0	5·0 ± 3·1	4·3 ± 1·2	5·2 ± 3·6	0·222	7·2 ± 4·4	6·6 ± 3·2	7·7 ± 5·3	0·319	**0·004**
Glucose (mg/dl)	94·1 ± 9·0	95·0 ± 9·2	92·5 ± 6·4	96·0 ± 9·9	0·156	93·3 ± 8·9	92·4 ± 9·9	94·1 ± 8·0	0·492	0·323
Leptin (ng/ml)	7·9 ± 6·2	4·4 ± 2·3	4·5 ± 1·3	4·3 ± 2·5	0·825	11·0 ± 6·9	10·2 ± 5·6	11·6 ± 8·0	0·440	**0·001**
HOMA-IR	1·4 ± 1·0	1·2 ± 0·8	1·0 ± 0·3	1·2 ± 0·9	0·136	1·7 ± 1·1	1·5 ± 0·7	1·8 ± 1·4	0·223	**0·007**
Systolic BP (mmHg)	140·2 ± 19·6	136·2 ± 19·5	145·8 ± 20·3	132·7 ± 18·3	0·055	143·7 ± 19·1	142·6 ± 20·2	144·6 ± 18·4	0·699	0·050
Diastolic BP (mmHg)	82·4 ± 10·4	81·0 ± 11·0	87·5 ± 10·0	78·7 ± 10·5	**0·014**	83·6 ± 9·8	85·7 ± 11·4	81·7 ± 7·9	0·141	0·215
Sleeping duration (h)***	6·7 ± 1·0	6·8 ± 1·3	6·7 ± 1·1	6·9 ± 1·3	0·594	6·6 ± 0·8	6·8 ± 0·7	6·5 ± 0·8	0·172	0·437

KPMC, Kyoto Preventive Medical Center; KUH, Kyoto University Hospital.
*KPMC vs KUH; **male vs female; ***information of one male subject in KUH is unknown.
Bold values: P<0·05.
Système International (SI) units for GH, micrograms per liter (conversion factor, 1·0); for IGF-1 to nanomoles per liter (0·131); for glucose, millimoles per liter (0·05551); for insulin, picomoles per liter (6·945); for leptin, nanomoles per liter (0·08).

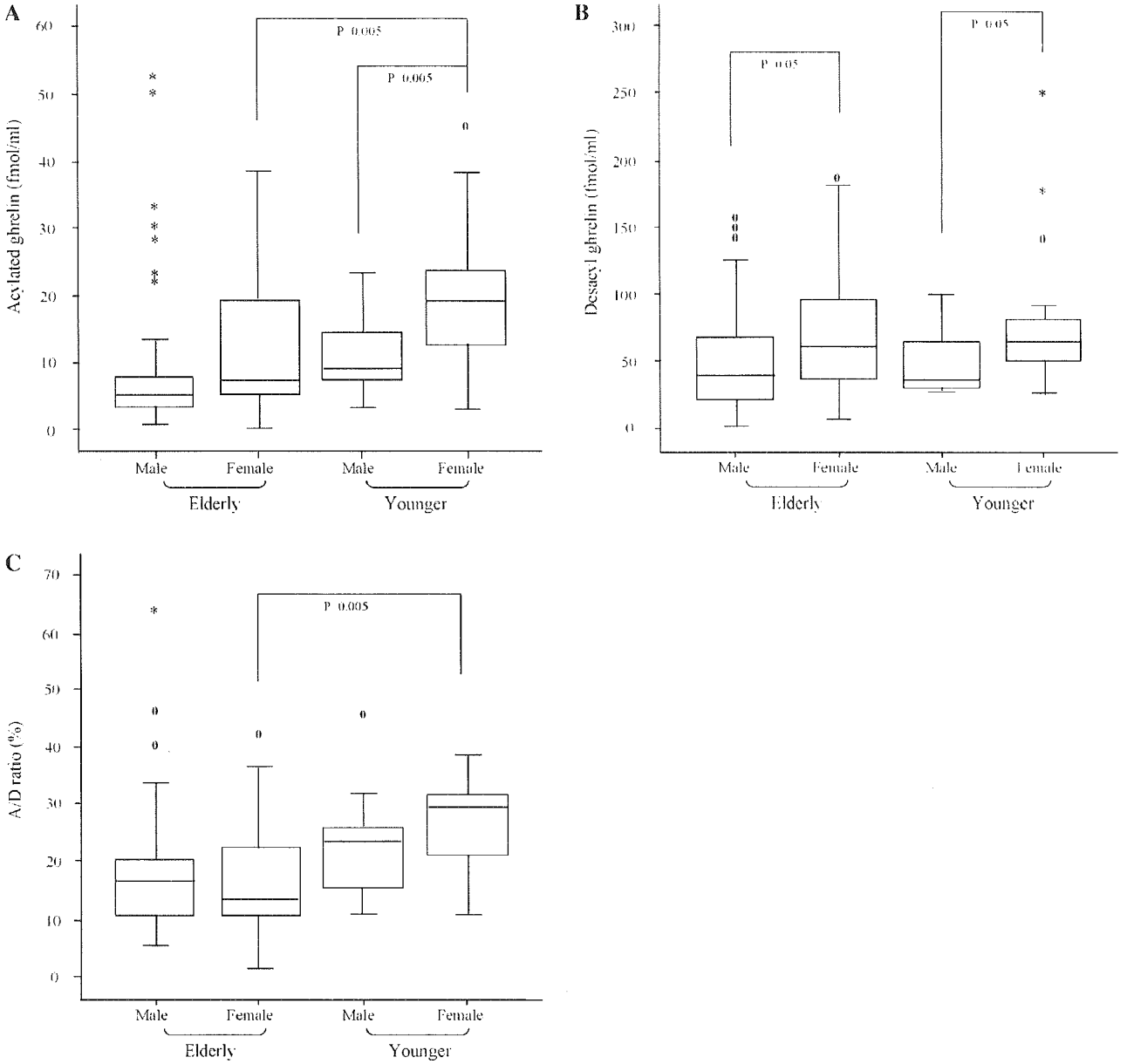

Figure 1 Comparison of plasma acylated ghrelin levels (A), desacyl ghrelin levels (B) and (C) A/D ratios between elderly and younger subjects. The values for subjects younger than 65 years are derived from our previous studies (Akamizu *et al.* 2005). Results are shown as box and whiskers plots. The upper hinge of the box represents the 75th and the lower the 25th percentile. The median is shown as a line across the box. The whiskers above and below the boxes represent the largest and smallest observed scores that are less than 1·5 box lengths from the box. Values farther away are potential outliers. If zero (0) appears, the value is between 1·5 and 3 interquartile ranges from the top or bottom edge of the box. If an asterisk (*) appears, the value is more extreme.

were not significantly different from those in younger female subjects. In addition, plasma levels of desacyl ghrelin in elderly subjects were not associated with gender (P=0·175). Although age and blood levels of GH and insulin were correlated with plasma levels of acylated and/or deacyl ghrelin in younger subjects, no parameter correlated with them in elderly subjects or elderly males. In elderly females, however, acylated ghrelin levels positively correlated with IGF-I (P=0·010). As this positive correlation between ghrelin and IGF-I levels was surprising, we examined the interaction between BMI and IGF-I by dividing female subjects into two groups based on the median value of BMI, 23·3. Acylated ghrelin levels correlated significantly with IGF-I levels in the group with lower (<23·3) (P=0·014), but not higher (>23·3) (P=0·090), BMI values (Fig. 2). We did not observe any

Table 2 Mulitiple regression analysis between plasma ghrelin concentrations and various parameters in healthy elderly and younger subjects

	All						**Elderly**											
	Male (n=65)			Female (n=76)			All (n=105)			Male (n=49)			Female (n=56)			**Younger*** (All) (n=36)		
	β	P	r^2 (%)	β	P	r^2 (%)	β	P	r^2 (%)	β	P	r^2 (%)	β	P	r^2 (%)	β	P	r^2 (%)
Acylated ghrelin																		
Site								0·172	0·433	0·7		0·076	0·831	0·1		0·540	0·087	6·2				
Gender								0·366	0·138	2·3									0·196	0·439	2·2
Age group	−0·184	0·661	0·3	0·047	0·914	<0·1		—	—	—		—	—		—	—		—	—	—	—
Age	—	—	—	—	—	—		0·001	0·957	<0·1		0·005	0·873	<0·1		−0·012	0·721	0·3		−0·044	**0·002**	31·0
BMI	−0·058	0·333	1·6	0·064	0·281	1·7		−0·026	0·621	0·3		−0·070	0·426	1·7		0·149	0·065	7·2		0·067	0·136	8·1
GH	0·003	0·906	<0·1	0·046	0·080	4·4		0·015	0·608	0·3		0·003	0·938	<0·1		0·094	0·123	5·1		0·036	**0·026**	17·1
IGF-I	0·003	0·204	2·8	0·006	**0·011**	9·2		0·006	0·113	2·7		0·003	0·588	0·8		0·015	**0·010**	13·6		0·001	0·523	1·5
Insulin	−0·032	0·374	1·4	−0·008	0·811	<0·1		−0·015	0·632	0·2		−0·024	0·657	0·5		−0·008	0·847	<0·1		−0·067	**0·015**	20·2
Glucose	−0·001	0·913	<0·1	0·008	0·559	0·5		0·000	0·988	<0·1		0·000	0·993	<0·1		0·008	0·619	0·5		−0·028	0·086	10·6
Leptin	0·015	0·796	0·1	−0·010	0·717	0·2		0·020	0·470	0·6		−0·009	0·920	<0·1		−0·052	0·176	3·9		−0·002	0·904	<0·1
Sleeping time								0·008	0·938	<0·1		0·030	0·813	0·1		0·157	0·369	1·8				
Desacyl ghrelin																		
Site	—	—	—	—	—	—		−0·317	0·102	2·8		−0·566	0·124	6·1		−0·044	0·858	<0·1		—	—	—
Gender								0·293	0·175	2·0										0·012	0·959	<0·1
Age group	0·076	0·858	<0·1	0·428	0·214	2·3																
Age								0·007	0·670	0·2		0·004	0·881	<0·1		0·015	0·550	0·8		0·014	0·231	5·3
BMI	−0·011	0·848	<0·1	0·022	0·646	0·3		−0·040	0·387	0·8		−0·046	0·604	0·7		0·047	0·457	1·2		0·034	0·409	2·5
GH	0·022	0·447	1·0	0·037	0·075	4·6		0·021	0·407	0·7		0·012	0·756	0·3		0·060	0·213	3·4		0·027	0·063	12·3
IGF-I	0·003	0·264	2·2	0·004	**0·024**	7·3		0·002	0·460	0·6		0·000	0·994	<0·1		0·008	0·094	6·0		0·001	0·467	2·0
Insulin	0·038	0·297	1·9	0·023	0·395	1·1		0·009	0·745	0·1		0·018	0·740	0·3		0·007	0·826	0·1		0·064	**0·013**	20·9
Glucose	0·010	0·475	0·9	0·010	0·340	1·3		0·006	0·573	0·3		0·002	0·937	<0·1		0·016	0·212	3·4		0·024	0·105	9·4
Leptin	0·018	0·766	0·2	0·003	0·903	<0·1		0·025	0·308	1·1		0·020	0·819	0·1		−0·014	0·634	0·5		0·005	0·772	0·3
Sleeping time	—	—	—	—	—	—		−0·036	0·667	0·2		−0·004	0·974	<0·1		−0·002	0·989	<0·1		—	—	—

Bold values: P<0·05.
β: regression coefficient.
r^2 (%): squared partial correlation coefficient.
*The number of younger subjects is too small to be stratified by gender for multiple regression analysis.